Available online at www.sciencedirect.com
ScienceDirect
Journal of Power Sources 171 (2007) 811–817
JOURNAL OF POWER SOURCES
www.elsevier.com/locate/jpowsour

Regeneration of an *n*-decanethiol-poisoned nickel catalyst

H. Oudghiri-Hassani [a], N. Abatzoglou [a,*], S. Rakass [a], P. Rowntree [b]

[a] *Department of Chemical Engineering, Université de Sherbrooke, 2500 Boul. Université, Sherbrooke, Quebec, Canada*
[b] *Department of Chemistry, University of Guelph, 50 Stone Road East, Guelph, Ontario, Canada N1G 2W1*

Received 11 May 2007; received in revised form 25 June 2007; accepted 26 June 2007
Available online 10 July 2007

Abstract

The regeneration of an *n*-decanethiol-poisoned nickel catalyst by treatment with steam was studied using diffuse reflectance infrared Fourier transform spectroscopy (DRIFTS), X-ray photoemission spectroscopy (XPS) and mass spectrometry (MS). The catalytic activity of a Ni catalyst contaminated with *n*-decanethiol ($H{-}(CH_2)_{10}{-}SH$) before and after regeneration was measured on methane steam reforming at a CH_4:H_2O ratio of 1:2 at 700 °C and compared to the nickel catalyst. The results show that, although (a) in the regenerated catalyst surface there is no residual sulfur and (b) the amount of surface carbon is the same as in Ni catalyst, the regenerated catalyst has gained 84% of its catalytic activity. Since all sulfur is removed, this loss of activity is attributed to structural changes at the surface of the catalyst and to the different nature of the remaining carbon.

Keywords: Regeneration; Steam reforming; Ni catalyst; Sulphur poisoning; XPS; IR

1. Introduction

Nickel continues to be both a well established and a promising new material in several developing fields of applied technology such as those arising in catalysis and in fuel cells [1,2]. For example, steam reforming, long used in the manufacture of synthesis gases and pure hydrogen from hydrocarbons, is a catalytic process involving ceramic-supported nickel catalysts. Coke formation [3–10] and sulfur poisoning [3,5,9,11,12] are two of the major problems associated with nickel catalysts. The presence of sulfur collecting on a catalyst surface is known to cause substantial losses of the catalyst's activity in many desired reactions, particularly those utilized in methane steam reforming processes [3]. This loss of activity is due to (1) direct sulfur adsorption on nickel particle surface(s) which hinders further adsorption of the reactant molecules and (2) the reconstruction of the Ni surfaces (i.e. sulfur can modify the chemical nature of the active Ni sites or result in the formation of new compounds which may modify or decrease the adsorption rates of reactant gases). The presence of carbon on catalyst surfaces can also cause (a) the blockage of desirable catalyst pores, (b) the loss of structural integrity of the catalyst support material [3,5,6,8] and (c) fouling of the catalysts surfaces. Catalyst deactivation may be overcome, at least partially, through timely regeneration processing.

Relatively few studies, on the regeneration of sulfur-poisoned and carbon-poisoned catalysts, have been reported in the literature. In the case of sulfur deposits, the following processes have been studied for their efficiency in the removal of sulfur from poisoned nickel catalysts and the restoration of their activity: (a) reduction with hydrogen [12,13] and (b) mild conditions oxidation, with oxygen or water [14,15]. The final goal is the removal of surface sulfur through H_2S or SO_2 formation. Efforts made to regenerate sulfur-poisoned Ni catalysts, using H_2 [15–17] alone, have been largely unsuccessful. One US Patent [18] proposes the use of H_2 to regenerate 15–60% Ni/Al_2O_3 at 700–1100 K, although reportedly, no sulfur is actually removed by this treatment. In respect of the study of regeneration using steam reaction, Rostrup-Nielsen [19] have reported that up to ~80% removal of the surface sulfur from Ni can be achieved at 700 °C, being either promoted or unpromoted by Mg and Ca, steam reforming catalysts. Aguinaga [13] had studied the regeneration of a nickel/silica catalyst, poisoned by thiophene, through oxidation–reduction treatments use, and they report that the sulfur removal efficiency of these methods is as high as 90% when they are applied to completely deactivated catalysts.

* Corresponding author. Tel.: +1 819 821 7904.
E-mail address: Nicolas.Abatzoglou@USherbrooke.ca (N. Abatzoglou).

0378-7753/$ – see front matter © 2007 Elsevier B.V. All rights reserved.
doi:10.1016/j.jpowsour.2007.06.258

In the case of undesirable surface carbons, the literature reports that they are generally highly reactive and may be gasified by means of reaction with hydrogen, carbon dioxide and/or steam, with nickel as the catalyst [20,21]. Bernardo [22] had studied the kinetics of the gasification removal of carbon, previously deposited on nickel catalysts, by means of carbon's reaction with (a) steam, (b) carbon dioxide and (c) hydrogen, at temperatures in the range of 450–850 °C. They reported that, for these particular reagents and at atmospheric pressure, steam is the most effective gasifying agent of the group.

The present text describes a study of the catalytic activity taking place during the steam reforming of methane over a pure Ni catalyst powder, pre-contaminated with *n*-decanethiol (H–$(CH_2)_{10}$–SH), both before and after the catalyst regeneration. In previously published work of the present authors [36,37] it has been shown that this Ni powder can be used effectively as a CH_4 steam reforming catalyst but related data regarding the sulfur and carbon poisoning sensitivity and the regeneration efficiency of such a catalyst, was not then available. The regeneration of the experimental catalyst was conducted in an oxidizing atmosphere, being confirmed by reference to data from infrared spectroscopy (IR) and X-ray photoemission spectroscopy (XPS).

2. Materials and methods

The catalyst used in this study was a very pure nickel powder. Ni powder of this quality is produced by the thermal decomposition of nickel tetracarbonyl [23] and is produced by the Inco Co. (Inco Ni 255). More details on this product can be found elsewhere [24]. The *n*-decanethiol (H–$(CH_2)_{10}$–SH) (Aldrich, 98%), and methanol solvent (Aldrich, 99%) employed in this work are both liquids at room temperature and were used in the as-received condition.

Thiol contamination of the Ni catalyst was achieved by prior immersion of the nickel powder catalyst into 10^{-3} M solutions of *n*-decanethiol/methanol (5 g of Ni in 100 ml of solution) at ambient temperature; these solutions contained several orders of magnitude excess thiol compared to the quantities constituting a monolayer on the Ni powder. The thiol immersion time was 20 h, after which, all such treated samples were rinsed with copious quantities of fresh methanol. Finally, the samples were dried for 12 h at ambient temperature and then used for the characterization and reforming tests. The decanethiol-contaminated Ni catalyst is hereafter denoted herein as Ni–$C_{10}S$. Diffuse reflectance infrared fourier transform spectroscopy (DRIFTS) was subsequently used to characterize all original and generated powders and pellets discussed in this paper, using a Nicolet Nexus 470 FTIR spectrometer. The resolution was set at 4 cm^{-1} and 256 scans were accumulated in an inert atmosphere at room temperature. The spectra were acquired using a MCT detector. X-ray photoelectron spectra (XPS) of the catalyst samples were acquired at ambient temperature, using a Kratos HS system, fitted with a monochromatized Al Kα ($h\nu$ = 1486.6 eV) X-ray source, and operated at 120 W; a 12 000 μm^2 region of the sample actually being probed. The photoelectron kinetic energies were measured using a hemispherical electrostatic analyzer, working in constant pass energy mode. The background pressure in the analysis chamber was maintained at below 2×10^{-8} Torr. Survey scans (0–1200 eV) and high-resolution Ni 3p, S 2p, C 1s and O 1s spectra were obtained at pass energies of 160 eV and 40 eV, respectively. Correction for charging effects was achieved by referencing all values of binding energies with respect to the O 1s core-level spectrum in NiO (BE ≈ 529.1 eV [25]). The uncertainty in the peak position was estimated to be ±0.2 eV for all spectra. The analysis of the measured Ni 3p, S 2p, C 1s and O 1s high-resolution spectra envelopes was performed by curve-fitting synthetic peak components, using XPSPEAK41. The raw experimental data were used without preliminary smoothing. Gaussian–Lorentzian product functions and Shirley background subtraction procedures were used to approximate the line shapes of the fitting components. Quantification of the carbon atomic percentages was obtained from the integration of the C 1s core-level spectra with application of the appropriate corrections for photo-ionization cross-sections. In this study, for each experiment, we tested at least two samples. For example, Fig. 1 shows the methane conversion for four experiments of steam reforming in the same conditions. These experiments use the same catalysts and they serve to prove the reproducibility and the statistical error of the reported results.

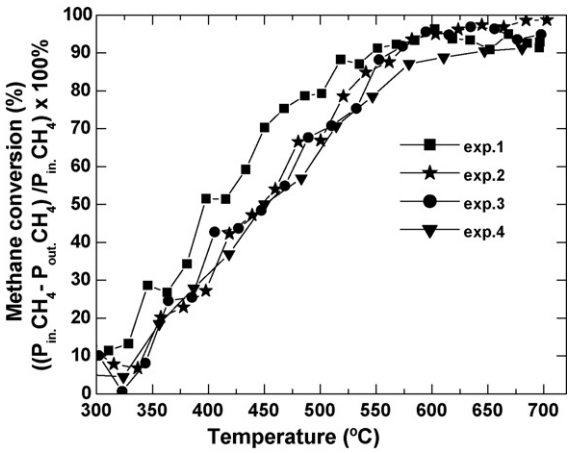

Fig. 1. Four reproducibility tests: methane conversion (%) over Ni catalyst as a function of temperature. Reaction conditions: $P(CH_4) = 10$ Torr, $P(H_2O) = 20$ Torr, $P(Ar) = 730$ Torr. CH_4 conversion is defined as follows: CH_4 conversion (%) = $((P_{in.CH_4} P_{out.CH_4})/P_{in.CH_4}) \times 100\%$.

The description of the experimental setup, and the protocols employed for the catalytic activity measurement, can be found elsewhere [24].

3. Results and discussions

3.1. Catalyst contamination

DRIFT data for the *n*-decanethiol adsorbed on Ni at ambient temperature in the C–H stretching bands were recorded and are presented in Fig. 2. The data show both methyl and methylene C–H stretching peaks. Mode assignments for each peak are also listed on the same figure. Peak positions are ~2850 cm^{-1} ($\upsilon_{symmetric}$, CH_2), ~2918 cm^{-1} ($\upsilon_{antisymmetric}$,

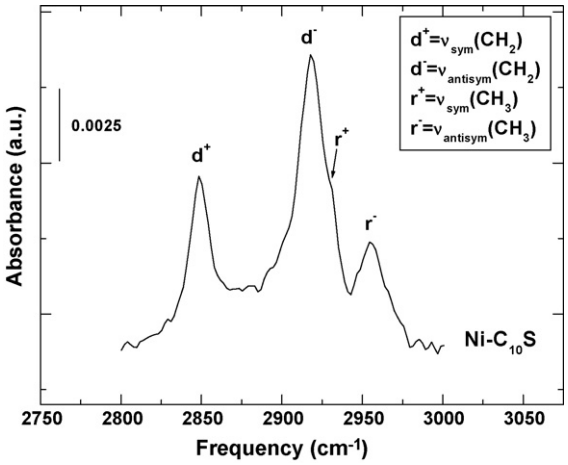

Fig. 2. DRIFTS spectra of the as-prepared decanethiol-contaminated Ni catalyst [37].

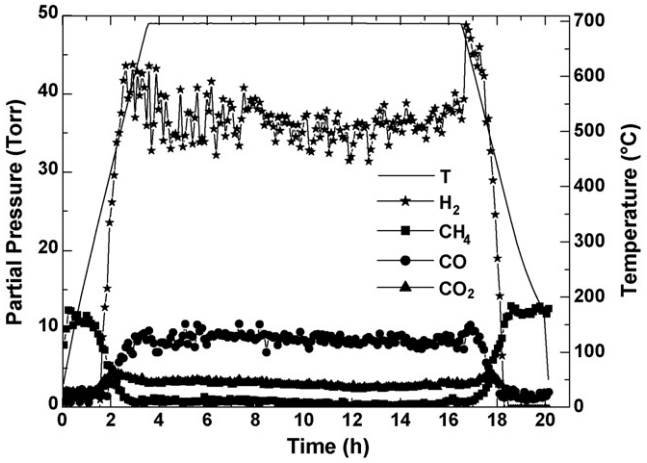

Fig. 4. Gas composition and temperature profiles vs. time on-stream for steam reforming with an unsupported Ni catalyst. Reaction conditions: $P(CH_4) = 10$ Torr, $P(H_2O) = 20$ Torr, and $P(Ar) = 730$ Torr.

CH_2), ~2930 cm^{-1} ($\upsilon_{symmetric}$, CH_3 FR^+) and ~2955 cm^{-1} ($\upsilon_{antisymmetric}$, CH_3), respectively [29,30]. The relative intensities of these various peaks, their peak positions and the peaks widths, are remarkably similar to those of alkanethiol monolayers, as adsorbed on planar Au(1 1 1) substrates [26,27], suggesting that the local environment for these adsorbates on the Ni surface is a rather well ordered one, despite the long-range disorder implicit in the use of powdered surface substrates. The spectra of the thiol-contaminated Ni powder did not exhibit significant intensity in the peak associated with the symmetric stretching mode of the terminal methyl groups (~2875 cm^{-1}). This result is similar to that obtained in the study of self-assembled monolayers, formed on metallic nanoparticules [28,29], for which this peak is either very weak or absent.

Fig. 3(a) and (b) shows the XPS spectra of the C 1s and S 2p binding energy regions, respectively, for decanethiol (Ni–$C_{10}S$). From an analysis of the near-surface atom compositions, the existence of two forms of sulfur S 2p, located at 162.7 eV and 168 eV, was confirmed (Fig. 3b). The first peak corresponds to thiolates [30–32], while, the second peak is typical of sulfonates [32,33]. This is in good agreement with the findings obtained in a study of the wetting properties for self-assembled monolayers of *n*-alkanethiols on copper surfaces [34]. In the case of the carbon C 1s spectral region (Fig. 3a), two peaks can be distinguished. The first peak, located at ≈288.7 eV, is attributed to C=O. This originates from the Ni catalyst powder, being commercially produced by the thermal decomposition of $Ni(CO)_4$ [23]. It is not known at this time if the residual chemisorbed CO affects the binding of the thiols to the Ni powders. The second peak, observed at ≈284.5 eV, is attributed to graphitic (i.e. aliphatic) carbon, originating from the decanethiols chemisorbed on the catalyst surface. This assignment is consistent with adsorbed thiolate [30,31,35].

The presence of the two sulfur chemical states, thiolates and sulfonates, on the catalyst surface, along with the CH_2 and CH_3 stretching bands (characterized by infrared spectroscopy, as described above), shows that the room-temperature adsorption of the *n*-decanethiol molecules takes place through the sulfur atom and not through the carbonaceous chain. Our XPS results corroborate with the DRIFTS results and confirm the adsorption of the decanethiols on the catalyst surface by the sulfur site [37].

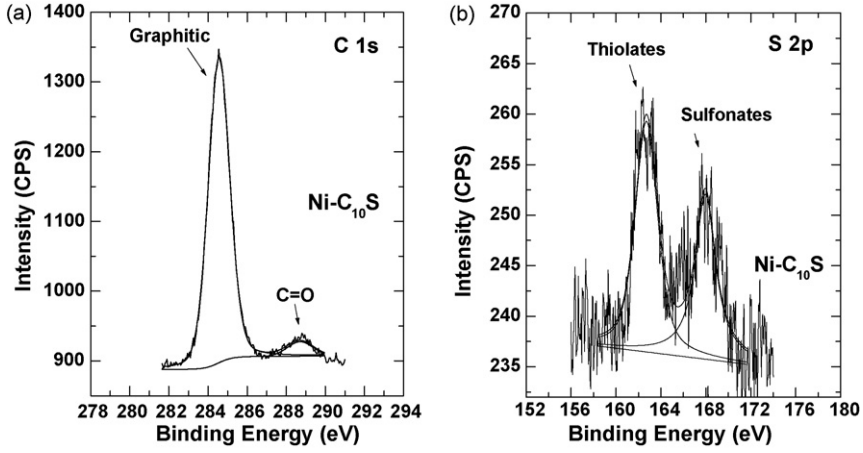

Fig. 3. XPS spectra (a) carbon C 1s and (b) sulfur S 2p of the as-prepared Ni–$C_{10}S$ catalyst [37].

3.2. Catalytic test

The steam reforming of methane ($CH_4 + 2H_2O \rightarrow CO_2 + 4H_2$, $CH_4 + H_2O \rightarrow CO + 3H_2$) was used to test the catalytic activity of the *n*-decanethiol-contaminated Ni catalyst, and was then compared to that of a Ni catalyst. The reforming tests, as described previously [24,36], were conducted at a CH_4/H_2O ratio of 1:2 to ensure chemical equilibrium and high conversion yields, whilst avoiding any limitations related to the reaction kinetics. Fig. 4 presents the partial pressures of H_2, CH_4, CO_2 and CO in the exit gas, over time and temperature. The onset of hydrogen production is at ~325 °C; H_2 production increases as the temperature increases, the maximum yield being obtained at 500 °C. As the temperature was increased, from 500 °C to 700 °C, hydrogen production remained constant and was stable for over 13 h at $T = 700$ °C. Fig. 5 shows the deactivation for the *n*-decanethiol-contaminated Ni catalyst. It is clearly seen that catalysts remain inactive at any temperature between ambient and 700 °C. In a previous study [37], the authors have shown that the deactivation is due mainly to carbon deposition of the "unsaturated" type.

Fig. 6 presents representative IR spectra for *n*-decanethiol, adsorbed on Ni, and tested for the steam reforming of methane. The data have being recorded at two different temperatures, 23 °C (*n*-decanethiol adsorbed on Ni), and 700 °C (same Ni after steam reforming at 700 °C). This data shows the existence of significant surface modifications occurring during the steam reforming of methane. An analysis of the possible assignment of the individual absorption bands to the corresponding bond configuration was undertaken. At low frequencies, the spectrum recorded at 23 °C shows the presence of bands characteristic of *n*-decanethiol adsorption on Ni (ν(C–S), $\delta(CH_2)$ and $\delta(CH_3)$), and the presence of sulfonates [37–41]. The IR spectra of the samples tested for methane steam reforming at 700 °C (exposure of 13 h at this temperature) show, in addition to the bands observed at 23 °C, the appearance of new bands, corresponding to characteristic groups of unsaturated compounds [38–41]. At high frequencies, the spectrum recorded at 700 °C shows the presence of bands $\nu(CH_2)$ and $\nu(CH_3)$ also present at 25 °C. The presence of the last two bands at 700 °C can be explained as follows: the heating of the decanethiol-impregnated Ni powder up to 700 °C during the reaction of steam reforming is characterized by the partial pyrolysis of the adsorbed layers. The pyrolysis proceeds through the creation of C_xH_y species at the surface of the Ni, precursors of C=C and aromatic groups through dehydrogenation. The pyrolysis products passivate more aggressively the Ni surface because the double and aromatic bonds geometry allows the molecules to lie parallel to the surface and thereby deactivate it much more efficiently than the linear saturated thiols, which are anchored vertically on the Ni surface. More details can be found in published work of the authors [42]. Fig. 7 presents IR spectra for Ni catalyst used for the steam reforming of methane. A comparison of Figs. 6 and 7 shows that all bands in Fig. 6 coming from *n*-decanethiol adsorbed on the Ni catalyst are absent in Fig. 7. It can be concluded that the catalytic deactivation was caused by high surface carbon coverage, and possibly, by the presence of sulfur also, as described previously [37].

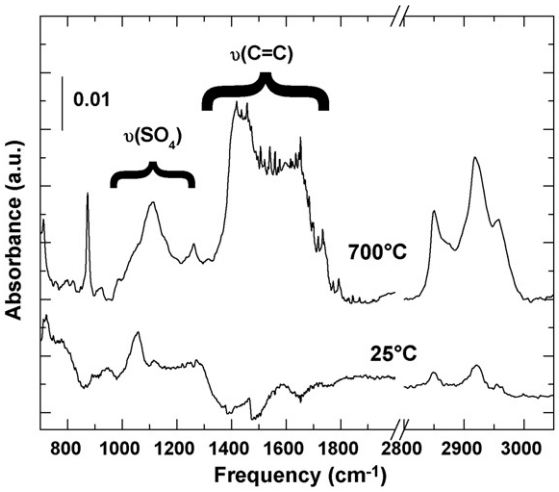

Fig. 6. DRIFTS spectra of Ni—C_{10}S recorded at 23 °C and 700 °C.

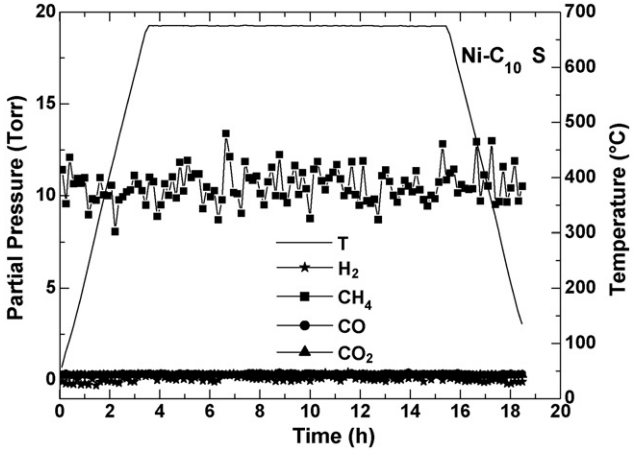

Fig. 5. Gas composition and temperature profiles vs. time on-stream for steam reforming with Ni—C_{10}S catalyst. Reaction conditions: $P(CH_4) = 10$ Torr, $P(H_2O) = 20$ Torr, and $P(Ar) = 730$ Torr.

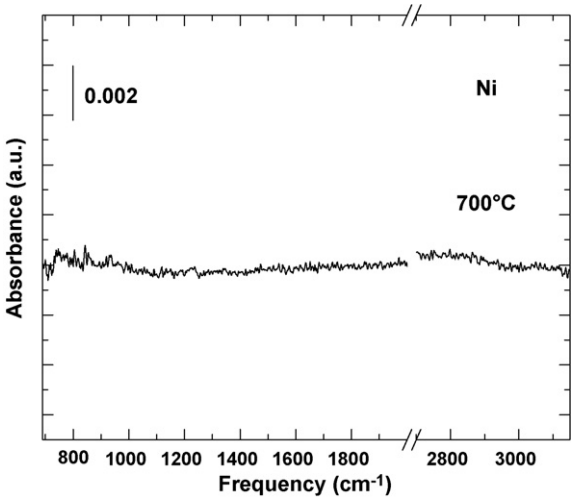

Fig. 7. DRIFTS spectra of Ni recorded at 700 °C after steam reforming.

3.3. Catalyst regeneration

The regeneration process was performed in an attempt to remove both carbon and sulfur from the Ni catalyst, using the steam treatment. The protocol involves a thermal treatment of the *n*-decanethiol-contaminated Ni catalyst up to 1050 °C (exposure of 0 h at this temperature) at a temperature ramp rate of 5 °C min^{-1} under a previously water saturated, pure Ar carrier gas. Water saturation was achieved by bubbling pure Ar through a controlled temperature water bath. Fig. 8 presents the DRIFTS spectrum of the thermally treated Ni catalysts surfaces. All previously observed bands associated with the *n*-decanethiol adsorbed on the Ni catalyst, tested for steam reforming of methane at 700 °C, disappear; and a new band, located at 1047 cm^{-1}, appears. The latter can be attributed to superoxo-species (Ni=O). Natile [43] had reported that the calcination of NiO powder at 973 K induces the appearance of a new peak at 1048 cm^{-1}, attributed to the formation of peroxo/superoxo-species.

The CH_4 catalytic steam reforming activity of the so treated catalyst was tested. Fig. 9 shows the activity of the *n*-decanethiol-contaminated Ni catalyst, treated by steam over time and temperature, by following the partial pressures of H_2, CO, CO_2 and CH_4. The onset of hydrogen production is now at about 500 °C instead of 325 °C for the Ni powder catalyst. H_2 production increases as temperature increases, and the maximum yield was obtained at 530 °C instead of the 500 °C value for the Ni powder catalyst. As the temperature increased from 530 °C to 800 °C, hydrogen production was constant, and remained stable for over 2 h at $T = 800$ °C. The methane conversion over Ni–C_{10}S treated in steam at $T = 700$ °C was 85 ± 2% compared to 94 ± 2% over the Ni catalyst and 100% for the theoretical prediction (thermodynamic equilibrium) (Fig. 10). The increased temperature for the onset of H_2 production, and the slight decrease of the methane conversion, relative to a Ni catalyst (e.g., the data of Figs. 4 and 10), seems to be due to the sintering of the loose Ni powder or to other structural changes. XPS analyses were carried out to confirm the cleansing of the catalyst surface.

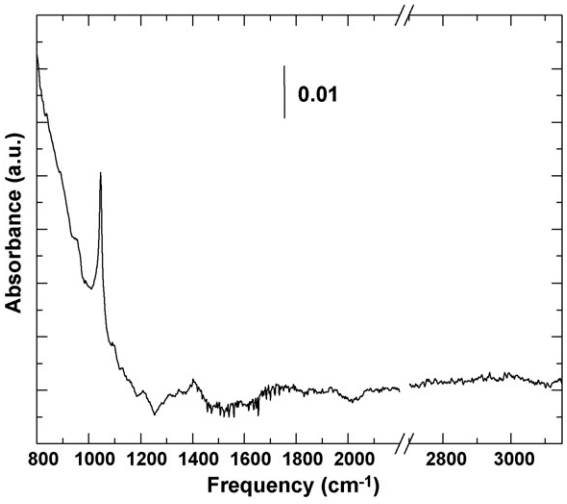

Fig. 8. DRIFTS spectra of Ni–C_{10}S after steam regeneration treatment as described in the text.

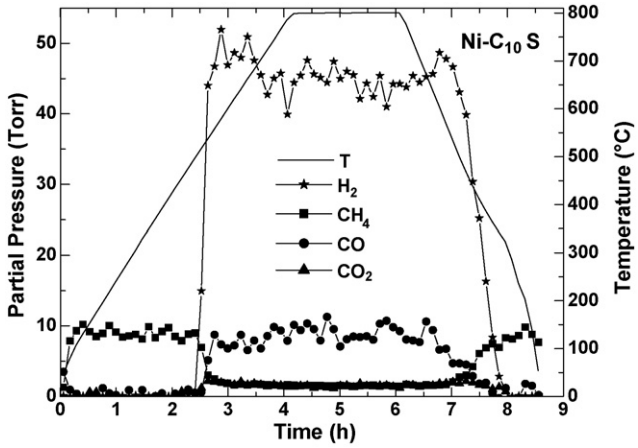

Fig. 9. Gas composition and temperature profiles vs. time on-stream for steam reforming with Ni–C_{10}S catalyst following the steam regeneration treatment. Reaction conditions: $P(CH_4) = 10$ Torr, $P(H_2O) = 20$ Torr, and $P(Ar) = 730$ Torr.

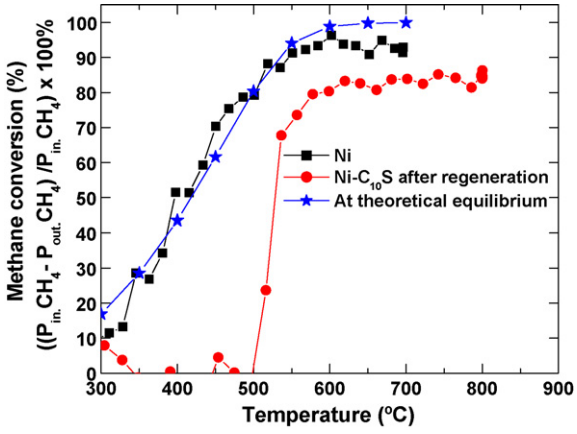

Fig. 10. Methane conversion (%) over Ni catalyst, Ni–C_{10}S catalyst following regeneration and at thermodynamic equilibrium during methane steam reforming, as a function of temperature. Reaction conditions: $P(CH_4) = 10$ Torr, $P(H_2O) = 20$ Torr, and $P(Ar) = 730$ Torr. CH_4 conversion is defined as follows: CH_4 conversion (%) = $((P_{in.CH_4} P_{out.CH_4})/P_{in.CH_4}) \times 100\%$.

Table 1 provides the relative intensities of the total carbon and the total sulfur with respect to the total Ni for: the nickel powder catalyst; the powder of Ni–C_{10}S; the Ni catalyst after 79 h in the steam reforming process at 700 °C; the Ni–C_{10}S after 13 h in steam reforming at 700 °C; the Ni–C_{10}S after its

Table 1
Area ratio of carbon and sulfur on nickel calculated for the various samples employed in this work

Catalyst sample	Relative C 1s intensities (%)	Relative S 2p intensities (%)
Nickel powder	58.5	0
Ni–C_{10}S powder	98.5	10.9
Ni catalyst after 79 h of steam reforming at 700 °C	27	0
Ni–C_{10}S catalyst after 13 h of steam reforming at 700 °C	59.5	5.1
Ni–C_{10}S catalyst after steam regeneration and steam reforming	25	0

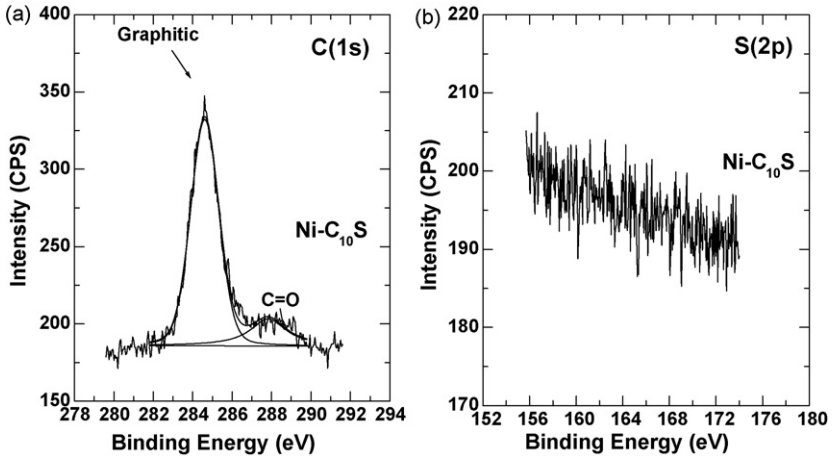

Fig. 11. XPS spectra (a) carbon C 1s and (b) sulfur S 2p of Ni–$C_{10}S$ catalyst after steam regeneration treatment.

steam treatment, followed by steam reforming. For the carbon, the coverage ratio of the Ni by carbon increases with the adsorption of the *n*-decanethiol on Ni; this coverage is 58.5% for Ni catalyst (due to atmospheric carbon) and 98.5% for Ni–$C_{10}S$. A decrease of the C 1s area coverage percentage from 58.5% to 27% and 98.5% to 59.5% after the use of steam reforming for both catalysts shows that there is little or no deposition of carbon in the case of Ni, and a partial elimination of carbon in the case of Ni–$C_{10}S$. However, in the case of Ni–$C_{10}S$ treated thermally in Ar/steam and followed by steam reforming, the C (s) area coverage percentage dropped to 25%; a value similar to that obtained after 79 h in steam reforming at 700 °C for the Ni catalyst. In the case of sulfur, the coverage ratio of the Ni by sulfur increases with the adsorption of the *n*-decanethiol on Ni; this coverage is 0% for powder of Ni and 10.9% for Ni–$C_{10}S$. A decrease of the S 2p area coverage percentage from 10.9% to 5.1% after the use of steam reforming for Ni–$C_{10}S$ catalysts shows a partial elimination of sulfur. However, in the case of Ni–$C_{10}S$ treated thermally in Ar/steam and followed by steam reforming, the S 2p area coverage percentage dropped to 0%. Besides, in the case of the Ni catalyst tested for 79 h in steam reforming conditions at 700 °C the area coverage percentage was 0% as expected. Fig. 11(a) and (b) shows the XPS spectra of the C 1s and S 2p binding energy regions, respectively, for Ni–$C_{10}S$ catalyst surface after its steam treatment. These results confirm that the treatment with steam on the Ni–$C_{10}S$ permits an apparently complete removal of the sulfur and a decrease of the area coverage percentage of the carbon from the catalyst. Nevertheless, it is not yet known whether the various carbon deposits (coverage) reported in this work are of the same nature. Thus, it is probable that, even if the carbon coverage percentage is the same, some types of carbon deposits are more prone to inhibit the catalytic activity than others.

4. Conclusion

In this paper, the topic of the steam regeneration of an unsupported Ni catalyst, contaminated with *n*-decanethiol, has been studied. The catalyst was obtained by immersion of the nickel powder in solutions of *n*-decanethiol/methanol at ambient temperature. The steam reforming of methane at a CH_4:H_2O ratio of 1:2 was employed to test the catalytic activity of the catalyst. The regeneration process is based on an oxidative removal of carbon and sulfur from the catalyst with heat treatment up to 1050 °C in steam. It was shown that, following its regeneration process, the catalyst has recovered some 84% of its catalytic activity. The surface analysis of the regenerated Ni powder surface shows that there was no residual sulfur, and that the quantity of the carbon present on the regenerated surface, reported as percentage of surface coverage by carbon, was similar to that obtained after 79 h in the steam reforming of the nickel catalyst at 700 °C. Since all sulfur is thereby removed, this loss of activity is attributed to structural changes at the surface of the catalyst. Finally, the nature of the carbon deposits must be further studied in order to understand whether its nature can also play an important role on the catalysts loss of activity.

Acknowledgements

The financial support of this work by NSERC (Natural Sciences and Engineering Research Council) and the CFI (Canadian Foundation for Innovation) is gratefully acknowledged. Special thanks to Gr. Peter Lanigan for reviewing the manuscript.

References

[1] F. Tietz, F.J. Dias, D. Simwonis, D. Stover, J. Eur. Ceram. Soc. 20 (2000) 1023.
[2] L. Daza, C.M. Rangel, J. Baranda, M.T. Casais, M.J. Martinez, J.A. Alonso, J. Power Sources 86 (2000) 329.
[3] J.R. Rostrup-Nielsen, J. Sehested, J.K. Norskov, Adv. Catal. 47 (2002) 65.
[4] H.S. Bengaard, J.K. Nørskov, J. Sehested, B.S. Clausen, L.P. Nielsen, A.M. Molenbroek, J.R. Rostrup-Nielsen, J. Catal. 209 (2002) 365.
[5] C.H. Bartholomew, Appl. Catal. A: Gen. 212 (2001) 17.
[6] P. Forzatti, L. Lietti, Catal. Today 52 (1999) 165.
[7] D.L. Trimm, Catal. Today 49 (1999) 3.
[8] D.L. Trimm, Catal. Today 37 (1997) 233.
[9] J.R. Rostrup-Nielsen, in: J.R. Anderson, M. Boudart (Eds.), Catalytic steam reforming in "Catalysis, Science and Technology", vol. 5, Sprimger-Verlag, Berlin, 1984 (chapter 1).
[10] J.R. Rostrup-Nielsen, J. Catal. 33 (1974) 184.

[11] J.R. Rostrup-Nielsen, J. Catal. 85 (1984) 31.
[12] C.H. Bartholomew, P.K. Agrawal, J.R. Katzer, Adv. Catal. 31 (1983) 135.
[13] A. Aguinaga, M. Montes, Appl. Catal. A 90 (1992) 131.
[14] H. Windawi, J.R. Katzer, Chem. Phys. Lett. 44 (1976) 332.
[15] H. Windawi, J.R. Katzer, J. Vac. Sci. Technol. 16 (2) (1979) 497.
[16] J.L. Oliphant, R.W. Fowler, R.B. Pannell, C.H. Bartholomew, J. Catal. 51 (1978) 229.
[17] C.H. Bartholomew, G.D. Weatherbee, G.A. Jarvi, J. Catal. 60 (1979) 257.
[18] H.H. Dobashi, US Patent 4,065,484, (1977).
[19] J.R. Rostrup-Nielsen, J. Catal. 21 (1971) 171.
[20] J.L. Figueiredo, D.L. Trimm, J. Catal. 40 (1975) 154.
[21] R.T.K. Baker, R.D. Sherwood, J. Catal. 70 (1981) 198.
[22] C. Bernardo, D.L. Trimm, Carbon 17 (1979) 115.
[23] F.V. Lenel, Powder Metallurgy, Principles and Applications, MPIF, Princeton, NJ, 1980, p. 40.
[24] S. Rakass, H. Oudghiri-Hassani, P. Rowntree, N. Abatzoglou, J. Power Sources 158 (2006) 485.
[25] K.S. Kim, R.E. Davis, J. Electron Spectrosc. Relat. Phenom. 1 (1973) 251.
[26] K.D. Truong, P. Rowntree, J. Phys. Chem. 100 (1996) 19917.
[27] C. Chung, M. Lee, J. Electroanal. Chem. 468 (1999) 91.
[28] S.W. Han, Y. Kim, K. Kim, J. Colloid Interf. Sci. 208 (1998) 272.
[29] M.J. Hostetler, J.J. Stokes, W. Murray, Langmuir 12 (1996) 3604.
[30] D.R. Huntley, J. Phys. Chem. 96 (1992) 4550.
[31] S.M. Kane, J.L. Gland, Surf. Sci. 468 (2000) 101.
[32] Z. Mekhalif, J. Riga, J.-J. Pireaux, J. Delhalle, Langmuir 13 (1997) 2285.
[33] Z. Mekhalif, F. Laffineur, N. Couturier, J. Delhalle, Langmuir 19 (2003) 637.
[34] P.E. Laibinis, G.M. Whitesides, D.L. Allara, Yu-T. Tao, A.N. Parikh, R.G. Nuzzo, J. Am. Chem. Soc. 113 (1991) 7152.
[35] T.S. Rufael, D.R. Huntley, D.R. Mullins, J.L. Gland, J. Phys. Chem. B 102 (1998) 3431.
[36] S. Rakass, P. Rowntree, N. Abatzoglou, Proceedings of Science in Thermal and Chemical Biomass Conversion, Victoria Conference Center and Fairmont Hotel, Victoria, Vancouver Island, BC, Canada, 30 August–2 September, 2004.
[37] S. Rakass, H. Oudghiri-Hassani, N. Abatzoglou, P. Rowntree, J. Power Sources 162 (2006) 579.
[38] M. Paronen, F. Sundholm, D. Ostrovskii, P. Jacobsson, G. Jeschke, E. Rauhala, P. Tikkanen, Chem. Mater. 15 (2003) 4447.
[39] G. Lazar, I. Lazar, J. Non-cryst. Solids 331 (2003) 70.
[40] V. Boiadjiev, A. Blumenfeld, J. Gutow, W.T. Tysoe, Chem. Mater. 12 (2000) 2604.
[41] B. Onida, L. Borello, C. Busco, P. Ugliengo, Y. Goto, S. Inagaki, E. Garrone, J. Phys. Chem. B 109 (2005) 11961.
[42] H. Oudghiri-Hassani, N. Abatzoglou, S. Rakass, P. Rowntree, in: C.A. Brebbia, V. Popov (Eds.), Energy and Sustainability, WIT Press, 2007, ISBN 978-1-84564-082-8, p. 177.
[43] M.M. Natile, A. Glisenti, Chem. Mater. 14 (2002) 4895.